Characterization of the (0001) cleavage surface of antimony single crystals using scanning probe microscopy: Atomic structure, vacancies, cleavage steps, and twinned interlayers

Bert Stegemann,* Claudia Ritter, Bernhard Kaiser, and Klaus Rademann
Institut für Chemie, Humboldt-Universität zu Berlin, Brook-Taylor-Strasse 2, D-12489 Berlin, Germany
(Received 19 September 2003; revised manuscript received 21 January 2004; published 30 April 2004)

Atomically resolved scanning tunneling microscopy images of the unreconstructed hexagonal structure of surface atoms on Sb(0001) are presented. Lateral and vertical lattice parameters have been determined. The interatomic spacing of 4.31 Å (± 0.05 Å) on the Sb(0001) surface corresponds to the known bulk data. Cleavage has been found to occur always between adjacent double layers, yielding at least diatomic cleavage steps of 3.75 Å (± 0.10 Å) height. Different kinds of defect structures on the cleavage plane have been imaged with atomic resolution. Point defects, caused by a single or by three missing surface atoms, have been uncovered. Stable imaging of cleavage steps, which were found to be straight along the atomic rows, has been achieved. Twinned interlayers formed upon cleavage of Sb even at room temperature have been revealed by atomic force microscopy. The mean twinning angle of 2.42° ($\pm 0.20°$) is quantitatively in accord with the value of 2.45° predicted by the model of twinning in Sb crystals. The observed features are discussed with respect to other layered materials and with regard to their relevance for the use of Sb(0001) as a support of nanostructures.

DOI: 10.1103/PhysRevB.69.155432 PACS number(s): 68.35.Bs, 68.35.Dv, 68.37.Ef, 68.37.Ps

INTRODUCTION

In recent years the formation of nanostructures on surfaces has been successfully accomplished, providing new insights into the understanding of the properties of low-dimensional structures and their technological applications. The self-organized growth of deposited atoms, clusters, or molecules has been reported to be highly efficient in this respect, since it allows the parallel and spontaneous assembly of nanostructured surfaces.[1–4] In particular, layered crystals provide excellent substrates for deposition and growth experiments, due to the various properties that make them outstanding in comparison with semiconductor or metal surfaces.[5] Layer-type materials are composed of layers held together only by weak van der Waals forces. Therefore, they can be cleaved easily, providing atomically flat surfaces which are ideal substrates with respect to the application of scanning probe microscopy (SPM) techniques.[6,7]

The most popular layered materials being employed in this respect include highly oriented pyrolytic graphite (HOPG) and the transition metal dichalcogenides (e.g., MoS_2, WSe_2). In contrast, the structurally related group V elements Sb and Bi, which are composed of layers as well and possess semimetallic properties, have still received little attention. While some SPM data of the basal (0001) cleavage plane of bismuth are available,[8–11] no real space investigation of the atomic scale properties of the basal plane of the lighter homologous and isostructural element antimony has been reported. Low-energy electron diffraction (LEED) experiments indicate that the Sb(0001) surface exhibits easy cleavage and is inert and thus reminiscent of the basal plane of HOPG.[12]

A prerequisite for the use of Sb(0001) as a substrate is a detailed knowledge of the regular atomic structure of the clean surface. Moreover, the recognition and elucidation of defect structures that can be produced by cleaving of Sb are important in order to distinguish these from actual structures formed during deposition and growth processes. In this respect a systematic investigation by means of SPM techniques is very promising, since it enables one to image surfaces in real space with atomic resolution and to probe minor surface heterogeneities that cannot be detected by averaging surface spectroscopy techniques.

In view of these facts a combined scanning tunneling microscopy (STM) and atomic force microscopy (AFM) study of the cleavage surface of Sb(0001) has been performed. The aim is to provide detailed reference data about the atomic scale properties of the basal plane and on surface imperfections, which can be found upon cleavage of Sb and which might be essential for a better understanding of growth processes on the surface. Particular emphasis is put on the atomically resolved study of vacancies and cleavage steps, and the identification of twinned interlayers.

Crystalline antimony has a rhombohedral structure[13] ($A7$, space group $R\bar{3}m$) and can be considered as a slightly distorted pseudocubic lattice. The lattice structure can best be visualized as a pile of atomic double layers stacked along the [0001] axis of a hexagonal basis. Each atom has three nearest neighbors within a double layer, three second-nearest neighbors in the adjacent double layer, and six third-nearest neighbor atoms within the hexagonal plane. Figure 1 depicts the hexagonal and the rhombohedral unit cell. The relevant lattice parameters are provided in Table I. In this text hexagonal notation will be adopted, as it is most convenient.

EXPERIMENT

Antimony single crystals were prepared from a melt of high-purity polycrystals (99.9999%) as follows:[14] The material was placed in a quartz test tube (diameter 8 mm), and then evacuated to 1×10^{-3} mbar and heated with a flame burner to the red glowing melt. Quenching of the melt in the test tube by cold water results in the formation of a single-

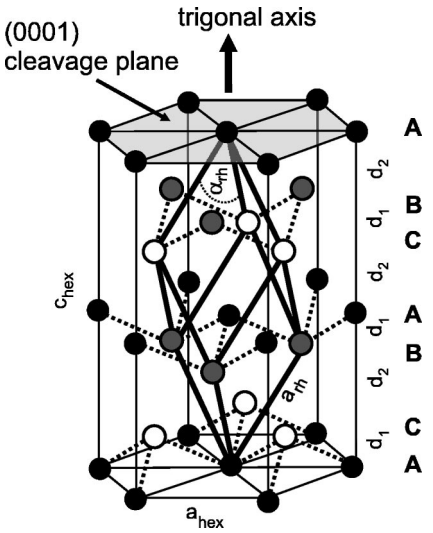

FIG. 1. Crystal lattice of antimony with rhombohedral and hexagonal unit cells. Atoms in layers *A*, *B*, and *C* are depicted in black, gray, and white, respectively. Refer to Table I for identification of the symbols.

crystal rod with a length of several centimeters. After removing the quartz glass it can be easily cleaved with a scalpel along the basal (0001) plane, which was found to be oriented perpendicular to the axis of the single crystal rod. X-ray Laue diffraction was employed in order to establish that the whole sample is a single crystal. For SPM analysis thin wafers with a (0001) surface were prepared at room temperature in air. After mounting on a substrate holder the samples were characterized with an AFM under ambient conditions or immediately transferred into an ultrahigh vacuum chamber (UHV, base pressure $<1\times10^{-10}$ mbar) for high-resolution analysis with the STM.

All AFM experiments have been performed with a home-built instrument[15] in the contact mode in air and at room temperature. Commercially available silicon cantilevers (length 450 μm, width 50 μm, thickness 2 μm, spring constant 0.2 N/m) were used. The AFM scanner unit is able to scan up to 240 μm$\times$240 μm. The *x*-*y* table and separate *z* piezo are equipped with integrated capacitive displacement sensors. Owing to the hardware linearized scanner unit thermal drift, nonlinearities ($<0.03\%$) and hysteresis are suppressed.

TABLE I. The lattice constants of antimony (Ref. 13).

Primitive rhombohedral cell	a_{rh}	4.5065 Å
	α_{rh}	57.11°
Hexagonal cell	a_{hex}	4.3081 Å
	c_{hex}	11.2737 Å
Pseudocubic cell	a_{pc}	6.2345 Å
	α_{pc}	87.42°
Nearest neighbor distance	a_{nn}	2.908 Å
Second nearest neighbor distance	$a_{2\mathrm{nn}}$	3.355 Å
Interplanar distance within a double layer	d_1	1.75 Å
Interplanar distance between double layers	d_2	2.00 Å

The UHV-STM is of the Beetle type designed by Besocke[16] and has a maximum scanning range of 500 nm $\times$500 nm. All STM data have been acquired at room temperature in the constant current mode using electrochemically etched tungsten tips. The *x*-*y* and *z* scales were calibrated on the basis of the lateral atomic structure of the (0001) basal plane of HOPG and of monatomic steps at the Au(111) plane, respectively.[17]

RESULTS AND DISCUSSION

Morphology and atomic structure of the cleavage plane

The Sb crystal produces a well-defined diffraction pattern with a trigonal symmetry, as verified by x-ray Laue diffraction. AFM analysis of the morphology of the surfaces as obtained by the cleavage reveals atomically flat terraces with a lateral extension of up to 10 μm. These terraces are separated by steps of different heights ranging typically from a few angstroms up to a few hundreds of nanometers. In Fig. 2(a) an atomically resolved STM image of a smooth terrace of the Sb(0001) cleavage plane is shown. A well-ordered arrangement of surface atoms with hexagonal symmetry is readily observed. For a detailed analysis of the interatomic distances and of the atomic corrugations the surface was imaged at higher magnification, as shown in Fig. 2(b). The surface profile along the line indicated in this STM image reveals equally corrugated and equally spaced maxima of the local density of states (LDOS) [Fig. 2(c)]. The measured corrugation amplitude at a tunneling gap resistance $R_T = 100$ MΩ is 0.5 Å ($\pm$0.1 Å). The distance between the maxima of the LDOS as measured from the STM images amounts to an average value of 4.31 Å ($\pm$0.05 Å), coinciding well with the expected value of 4.31 Å of the interatomic spacing in the (0001) basal plane of the Sb crystal (Fig. 1). Accordingly, the STM images of the cleavage surface reveal the true hexagonal configuration of the atoms of the Sb (0001) plane without reconstruction.

It should be noted that atomic resolution has been established without any cleaning treatment of the Sb(0001) surface under UHV conditions. This fact is in accordance with investigations on the reactivity of the Sb(0001) surface by element-specific surface analytical techniques like LEED (Ref. 12) and Auger electron spectroscopy.[18] There it was found that this surface is chemically stable and rather inert with respect to the adsorption of oxygen or water.

Structures on the cleavage plane

STM and AFM have also been applied to study crystal imperfections and cleavage induced structures on Sb(0001). The different phenomena that were frequently observed can be classified according to their dimensionality as follows: (i) vacancies (i.e., quasi-zero-dimensional defects), (ii) cleavage steps and edges at the onset of a new terrace (i.e., one-dimensional defects) and (iii) twinned interlayers (i.e., two-dimensional defects).

Vacancies

The atomic scale imaging of point defects is an important indication for the achievement of true atomic resolution;[19]

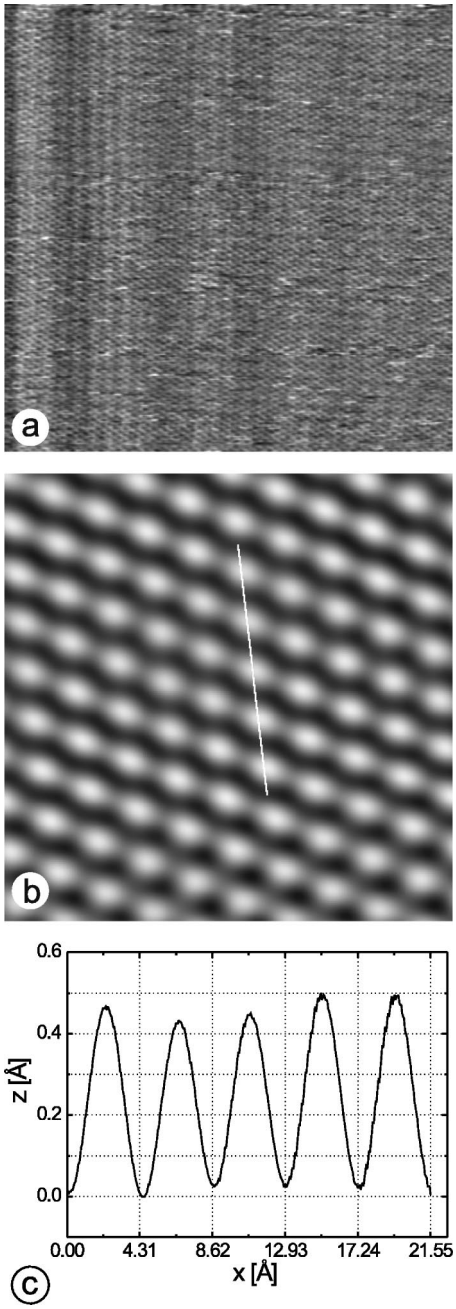

FIG. 2. STM topographs resolving the hexagonal arrangement of Sb atoms on the Sb(0001) surface. (a) 310 Å$\times$310 Å, tip bias 0.12 V, current 1.0 nA. Slight periodic height variations originate from vibrations during image acquisition. (b) 39 Å$\times$39 Å, tip bias 0.16 V, current 1.0 nA. A low-pass two-dimensional (2D) fast Fourier transform (FFT) filter has been applied in order to minimize noise. (c) Cross section according to the white line in (b) yielding a mean lattice constant of 4.31 Å and an atomic corrugation of about 0.5 Å.

however, it has turned out to be a challenging task. Although, e.g., HOPG has been extensively studied, only a few STM/AFM images of point defects of untreated HOPG(0001) have been shown. This lack of point defects is considered to be a problem of imaging rather than a question of their existence and has led to a controversial discussion of the imaging mechanism.[19]

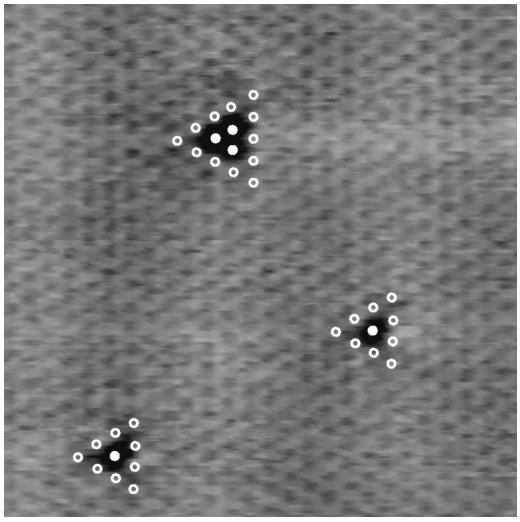

FIG. 3. STM topograph (100 Å$\times$100 Å) of vacancies on the (0001) cleavage plane. Tip bias -0.10 V, current 1.0 nA. The positions of the edge atoms and the missing atoms are marked with open and full circles, respectively.

Figure 3 clearly demonstrates that point defects on Sb(0001) can be atomically resolved with the STM. In this image three randomly distributed vacancylike features are detected on a 100 Å$\times$100 Å scale. The apparent positions of the edge atoms and the missing atoms are indicated with open and full circles, respectively. This designation allows the assignment of the two small pits to single-atom vacancies, whereas the larger triangular defect can be attributed to a triatomic vacancy. In contrast to observations on HOPG,[20] no indication of superlattice patterns or electronic perturbations in the STM image caused by the presence of such defects has been found.

Vacancy defects in the basal plane are of general interest due to their role as pinning and nucleation centers for mobile species on the surface.[21,22] Moreover, they act as active sites in chemical interactions, as it is known that vacancies on HOPG(0001) initiate oxidation reactions when exposed to molecular oxygen at elevated temperatures.[23] On Sb(0001) the vaporization was found to start at vacancy sites.[24] As the gas phase of antimony consists predominantly of Sb_4 molecules, vacancy sites are closely associated with the considerable structural rearrangement of bond distances and angles to form regular tetrahedral Sb_4 molecules[25] (bond length 2.687 Å, Sb-Sb-Sb bond angle 60°) from the rhombohedral lattice. However, the microscopic processes involved in this transformation are still under investigation.

Cleavage steps

Cleavage steps are the most frequently encountered structures on layered substrates. They are important in epitaxy and adsorption due to their higher-coordinated positions on the surface. These steps are known to occur mostly perpendicular to the cleavage direction, as demonstrated on HOPG,[26] and are characterized by the height of the steps, which is a multiple of the interplanar distance of the material. Shown in Fig. 4(a) is a STM image of a region of the

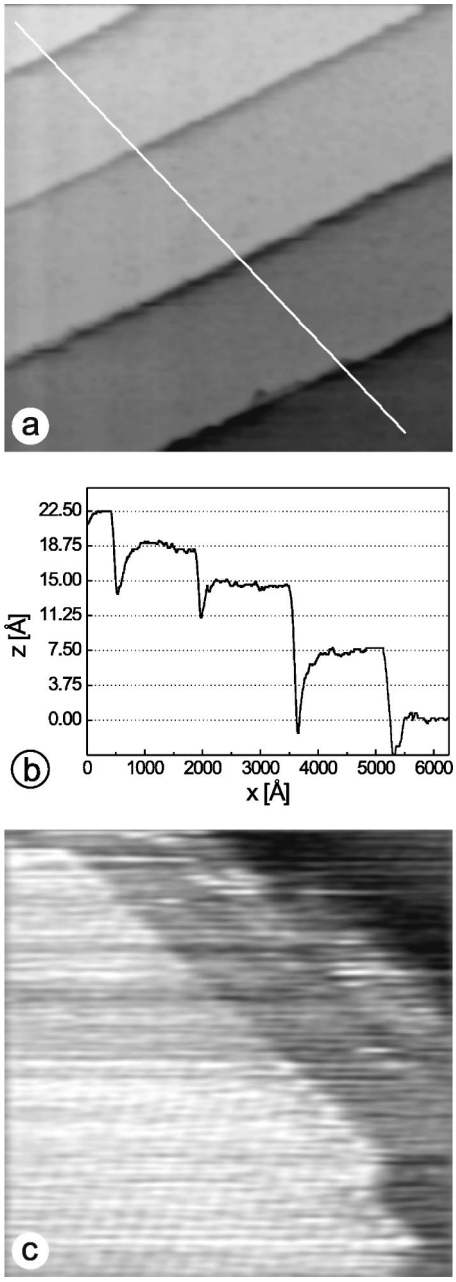

FIG. 4. (a) STM topograph (4960 Å×4960 Å) displaying atomically smooth, parallel terraces. Tip bias 0.05 V, current 1.0 nA. (b) Cross section of the boundary steps as indicated in (a). Trenches along the lower side of the steps are artifacts and due to the slow response of the feedback loop. (c) STM topograph (102 Å×102 Å, low-pass 2D FFT filtered) of a step edge at atomic resolution. Tip bias 0.10 V, current 1.0 nA.

Sb(0001) surface, where closely spaced cleavage steps are found. These straight steps are parallel to each other and form narrow, atomically smooth terraces with a width of about 1500 Å. The cross section in Fig. 4(b) reveals average step heights of 3.75 Å or 7.50 Å (±0.10 Å). These values can be explained as follows: As illustrated in Figs. 1 and 5 the double layer structure of the antimony crystal is based on atomic layers, which are separated by alternating distances of $d_1 = 1.75$ Å and $d_2 = 2.00$ Å. The smaller distance corresponds to mainly covalent bonds and hence leads to double layer formation, whereas between the distant layers, i.e., between neighboring double layers, van der Waals bonds prevail.[12] As a consequence, cleavage always occurs between neighboring double layers, resulting in step heights of 3.75 Å and multiples of this value.

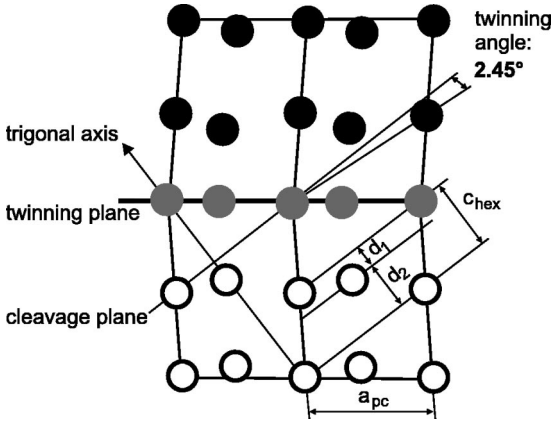

FIG. 5. (a) Illustration of a twin structure in antimony according to the model given in Ref. 27. The twinning angle is 2.45°. Refer to Table I for identification of the symbols.

Figure 4(c) reveals atomically resolved details of a step and its vicinity. The boundary of the terrace is close to the straight line of the atomic row. The hexagonal pattern and the atomic spacing near the step are not changed by the existence of the step. However, the corrugation of the atomic row at the edge appears slightly enhanced with respect to the normal corrugation, possibly due to dangling bonds at the edge. The stable imaging of the edge atoms is remarkable, since in the case of the (0001) surface of the heavier homologous element bismuth the terrace edges appeared blurred in the STM image.[9]

Twinned interlayers

Unexpectedly, twinned interlayers have been observed upon cleavage of Sb even at room temperature. It is known that there are two means of forming twins in metals, namely, the application of stress or heat.[27] The formation of twins in Sb single crystals due to plastic deformation by torsional stress[28] and by the indentor method,[29] and due to laser-induced deformation[30] was demonstrated several decades ago by optical studies. Recent developments like the nanoindentation technique have opened new possibilities and allow determination of the duration of the twinning process.[31] Moreover, the establishment of SPM techniques facilitates the investigation of natural twins on cleavage planes and their nanoscale properties, as has been demonstrated by the results on twinning in bismuth crystals at a low-temperature cleavage.[10,11]

The model of twinning in rhombohedral crystals is illustrated in Fig. 5.[27] The open circles represent the positions of the atoms in the untwinned region, the black circles the position in the twinned region. It is seen that the twinned and untwinned parts of the crystal are mirror reflections of each other in the twinning plane (gray circles). The twinning plane crosses the (0001) surface along the atomic rows. Following

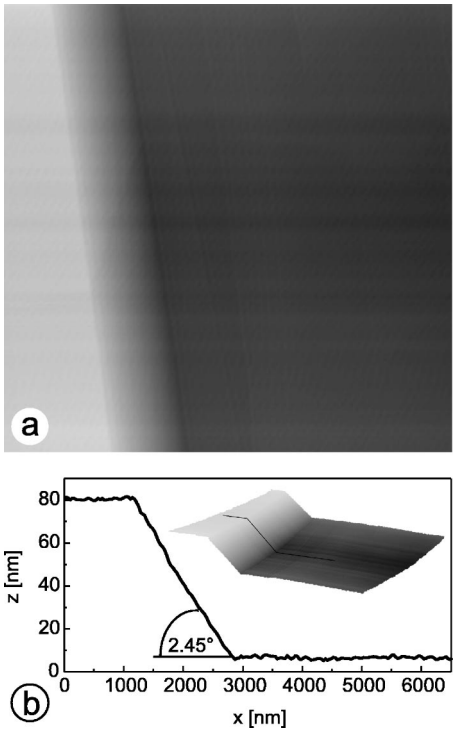

FIG. 6. (a) AFM topograph ($10\ \mu m \times 10\ \mu m$, height range 85 nm) of the Sb cleavage plane with two parallel terraces and a twinned interlayer. (b) Cross section along the line in the inset, which represents the three-dimensional visualization of the topograph in (a). The twinning angle is measured to be 2.45° (note the different scaling of the horizontal and vertical axes).

this model, the angular deviation of the inclined region with respect to the trigonal Sb cleavage plane (i.e., the twinning angle) can be calculated, and amounts to 2.45°.

Accordingly, in SPM topographs twinned structures on the Sb cleavage plane are recognized by two atomically smooth planes forming dihedral angles of either $(180 - 2.45)°$ or $(180 + 2.45)°$. These characteristic angles allow a clear distinction from regular step edges found at the onset of a conventional terrace. A typical example is shown in the AFM image of a surface region, which can be clearly identified as a twinned interlayer that is embedded in the main crystal [Fig. 6(a)]. As seen in the cross section given in Fig. 6(b) the surfaces on the right and on the left of the twinned interlayer are parallel to each other. The interlayer is characterized by a decline, i.e., it is tilted with respect to these planes. The twinning angle is determined to be 2.45°, matching the value proposed by the model. In our investigation 30 twin structures have been analyzed on numerous samples with regard to their angle and width. The twinned interlayers were found to be of different width ranging from 50 nm up to several micrometers. The twinning angle turned out to be constant within a range from 2.23° to 2.62°, resulting in a mean value of 2.42°, and thus being in excellent agreement with the calculated angle.

Natural twinned interlayers have not yet been detected by SPM at room temperature. Previous observations were made from twinned interlayers in bismuth which were cleaved at liquid nitrogen or liquid helium temperatures.[10,11] It has been stated that twinning facilitates the relaxation of stress occurring during cleavage of the crystal. However, in the case of Bi elevated temperatures lead to the annealing of the cleavage-induced stress and crystal defects. The lower ductility of Sb in contrast to Bi most likely explains the occurrence of natural twins on the cleavage plane at room temperature.

CONCLUSIONS

Morphology, atomic structure, and different kinds of defect structures of the basal plane of antimony single crystals have been explored in detail by a combined STM/AFM study. The most significant findings that result from this study are summarized as follows.

(i) Sb crystals were found to exhibit easy cleavage parallel to the (0001) plane due to their layered structure revealing large, atomically smooth terraces extending over many square microns. (ii) On these cleavage surfaces the true hexagonal lattice structure with a spacing of 4.31 Å (± 0.05 Å) is imaged, agreeing well with the bulk structure of Sb. The surface is fairly inert when exposed to air and remains unreconstructed. (iii) The amplitude of atomic corrugation is measured to be 0.5 Å (± 0.1 Å) at intermediate tip-sample distances. (iv) Atomic vacancies have been examined in atomically resolved STM images revealing single-atom vacancies and triangular pits of three missing surface atoms. (v) Cleavage results in the formation of boundary steps with a height of multiples of 3.75 Å (± 0.10 Å), coinciding with 1/3 of the hexagonal unit cell along the trigonal axis. Thus, cleavage occurs exclusively between adjacent double layers of the Sb crystal, resulting in at least diatomic cleavage steps. In contrast to the heavier homologous element Bi, stable imaging of the step edge atoms has been achieved. (vi) Twinned interlayers have been identified, which are characterized by a tilt of 2.45° with respect to the main crystal surfaces. This value is derived from the known model of twinning and is consistently found for all investigated twinned structures ($2.42° \pm 0.20°$). Contrary to previous work on Bi, the formation of natural twinned interlayers is evidenced even at room temperature, apparently originating from the lower ductility of Sb.

These results extend the database available on atomically resolved elemental surfaces and affirm the fundamental association with structurally related layered materials like HOPG and Bi at the atomic level. Furthermore, it has been demonstrated that Sb(0001) provides a well-defined, extended, and atomically flat surface, suitable as substrate for the investigation of growth processes, the synthesis of nanostructured surfaces, and nanomanipulation experiments.

ACKNOWLEDGMENTS

The authors are grateful to J. Opitz-Coutureau for the preparation of the antimony crystal, to J. Richter and R. Köhler for the x-ray analysis, and to T. M. Bernhardt for helpful discussions. This work has been supported by the Deutsche Forschungsgemeinschaft (DFG) and the Fonds der Chemischen Industrie.

*Present address: Institut für Experimentalphysik, Freie Universität Berlin, Arnimallee 14, D-14195 Berlin, Germany. Email address: bert.stegemann@berlin.de

[1] H. Brune, C. Romainczyk, H. Röder, and K. Kern, Nature (London) **369**, 469 (1994).
[2] P. Jensen, Rev. Mod. Phys. **71**, 1695 (1999).
[3] *Metal Clusters at Surfaces: Structure, Quantum Properties, Physical Chemistry*, edited by K.-H. Meiwes-Broer (Springer-Verlag, Berlin, 2000).
[4] B. Kaiser and B. Stegemann, ChemPhysChem **5**, 37 (2004).
[5] R. M. A. Lieth (ed.), *Preparation and Crystal Growth of Materials with Layered Structures* (Reidel, Dordrecht, 1977).
[6] C. J. Chen, *Introduction to Scanning Tunneling Microscopy* (Oxford University Press, New York, 1993).
[7] R. Wiesendanger, *Scanning Probe Microscopy and Spectroscopy: Methods and Applications* (Cambridge University Press, Cambridge, U.K., 1994).
[8] A. M. Troyanovskii and V. S. Edelman, JETP Lett. **60**, 300 (1994).
[9] A. M. Troyanovskii and V. S. Edelman, JETP Lett. **60**, 111 (1994).
[10] V. S. Edelman, Phys. Lett. A **210**, 105 (1996).
[11] V. S. Edelman, D. Y. Sharvin, I. N. Khlyustikov, and A. M. Troyanovskii, Europhys. Lett. **34**, 115 (1996).
[12] F. Jona, Surf. Sci. **8**, 57 (1967).
[13] J. Donohue, *The Structures of the Elements* (Wiley-Interscience, New York, 1974).
[14] J. Opitz-Coutureau, Ph.D. thesis, Humboldt-Universität zu Berlin, 2004.
[15] C. Ritter, M. Heyde, U. D. Schwarz, and K. Rademann, Langmuir **18**, 7798 (2002).
[16] K. Besocke, Surf. Sci. **181**, 145 (1987).
[17] B. Stegemann, *Wechselwirkungen monodisperser Antimon-Cluster mit Oberflächen: Diffusion, Wachstum und Struktur bildung im Nanometerbereich* (Shaker Verlag, Aachen, 2003).
[18] P. Ma and A. J. Slavin, Phys. Rev. B **49**, 8340 (1994).
[19] F. Atamny, O. Spillecke, and R. Schlögl, Phys. Chem. Chem. Phys. **1**, 4113 (1999).
[20] J. R. Hahn and H. Kang, Phys. Rev. B **60**, 6007 (1999).
[21] J. G. Kushmerick and P. S. Weiss, J. Phys. Chem. B **102**, 10094 (1998).
[22] S. J. Carroll, S. Pratontep, M. Streun, R. E. Palmer, S. Hobday, and R. Smith, J. Chem. Phys. **113**, 7723 (2000).
[23] S. M. Lee, Y. H. Lee, Y. G. Hwang, J. R. Hahn, and H. Kang, Phys. Rev. Lett. **82**, 217 (1999).
[24] G. M. Rosenblatt and P. K. Lee, J. Chem. Phys. **52**, 1454 (1970).
[25] V. Kumar, Phys. Rev. B **48**, 8470 (1993).
[26] H. Chang and A. J. Bard, Langmuir **7**, 1143 (1991).
[27] E. O. Hall, *Twinning and Diffusionless Transformations in Metals* (Butterworths Scientific Publications, London, 1954).
[28] H. J. Gough and H. L. Cox, Proc. R. Soc. London, Ser. A **127**, 431 (1930).
[29] K. Meyer and U. Brueckner, Krist. Tech. **1**, 477 (1966).
[30] K. Meyer and W. Meier, Krist. Tech. **3**, 399 (1968).
[31] O. M. Ostrikov and S. N. Dub, J. Eng. Phys. Thermophys. **76**, 200 (2003).